DINAME 2023 - Proceedings of the XIX International Symposium on Dynamic Problems of Mechanics,
A.S. De Paula, A.T. Fabro and M.R. Machado (Editors), ABCM.
Pirenópolis, Go, Brazil, February 26th to March 3rd, 2023

Damage Detection using GP-NARX models

André Vila Nova Mazzoni[1], **and Luis Gustavo Giacon Villani**[2]

[1,2] Departamento de Engenharia Mecânica, Centro Tecnológico, Universidade Federal do Espírito Santo – UFES, Av. Fernando Ferrari, 514, Vitória, Espírito Santo, Brasil.

Abstract: Damage detection is the first and main step in applying Structural Health Monitoring (SHM) procedures. Vibration-based damage detection methods are commonly applied because the signals are affected by structural changes, related to the structural dynamics. Usually, signals measured with the structure operating in unknown conditions are compared with reference signals predicted using baseline models. This step is not trivial when the structure to be monitored operates in a nonlinear regime of motion because linear models lose the capability to predict the baseline-dynamic behavior, inducing the false-positive occurrence, i.e., the confusion between the presence of damage and the presence of nonlinear phenomena. To overcome this issue this work proposes the use of a GP-NARX nonlinear model as a baseline model for structure monitoring. The GP-NARX model is constructed using the Gaussian Process (GP) machine learning method considering the framework of a Nonlinear Autoregressive with an eXogenous (NARX) input model. The advantage of doing so is the natural capability of calculating the model uncertainty, related to the GP model, and the versatility to describe various types of nonlinearities with minor changes in the model structure. The procedure was implemented considering simulated data, demonstrating the advantages of using the GP-NARX model for monitoring structures that can operate in a nonlinear motion regime.

Keywords: Damage detection, Nonlinear behavior, GP-NARX models, Structural Health Monitoring.

INTRODUCTION

Damage detection procedure applied to intrinsically nonlinear dynamic systems is not trivial. The fact that structures with nonlinear dynamics can change behavior simply by varying the amplitudes of the excitation forces (or type of force applied) can make structure monitoring based on linear reference models ineffective. In this situation, the behavior variation related to the nonlinear dynamics will be possibly confused with the presence of structural changes. Therefore, the use of nonlinear models becomes essential to ensure the good performance of reference model-based methodologies. Several types of models can be considered, each with its challenges, advantages, and disadvantages, whereby a good insight into their functionality can be found in Worden et al. (2007); Kerschen et al. (2007). In this context, several regression models that consider kernel-based machine learning models can be used in nonlinear system identification.

The Nonlinear Autoregressive with an eXogenous (NARX) input models are well known in the literature (Billings, 2013). The ability to represent the system output as a function of past inputs and outputs, considering nonlinear relations between them, is very interesting because it allows nonlinearities to be described without knowledge of all the physics involved in the phenomenon. The greatest difficulty in estimating such models is related to determining the nonlinear relationship between the past samples. At this point, the Gaussian Process regression machine learning model can be used together with the NARX framework, building the model known as GP-NARX. The main advantages are related to the Bayesian characteristic of the GP model, its ability to naturally estimate the uncertainties in the predicted output, and the need to estimate only the maximum number of lags used to build the model and not the individual relationships between each delay as in the classical NARX model version (Worden et al., 2018).

Hence, it becomes natural to think about using the GP-NARX model in damage detection problems in intrinsically nonlinear structures. This article represents a first step on that path. The main idea is to study the model's ability to predict the output signal of a nonlinear system considering different types of input force and different excitation amplitudes. Knowing that machine learning models can be great interpolators, but have difficulty extrapolating to conditions far from those under which they were trained (using available data), would it be possible to establish reliable operating ranges? This manuscript seeks to study the effect of increasing the nonlinear contributions in the total response of the systems on the performance of the model used, particularly in the context of damage detection.

Furthermore, it is necessary to construct a monitoring index that is able to compare new measured experimental signals with the reference model prediction, taking advantage of the model's ability to estimate confidence bands for the prediction made. The index has to be able to compensate for regions with high uncertainty, by giving low weight to prediction errors observed in these regions. As the GP-NARX model output includes estimated mean and variance, we propose using a distance metric that incorporates a variance normalization, based on standardized Euclidian distance. This is a simple way to take advantage of the main properties of the estimated prediction model. The idea is that prediction errors observed in regions where the model is more uncertain have lower contribution to the value of the damage index.

For doing so, the methodology proposed by the authors is applied considering the classic Duffing oscillator as a benchmark (Kovacic and Brennan, 2011). This benchmark has already been used extensively to describe the nonlinear behavior of numerous real structures. In addition, the use of simulated data allows further study of the influence of different operating conditions on the performance of the proposed method. The results show that the use of the GP-NARX model in combination with a distance metric is promising in the scope of damage detection in nonlinear structures. However, the user should be aware of the model's limitations regarding its performance under conditions far removed from those under which it was estimated.

DAMAGE DETECTION BASED ON GP-NARX MODEL

GP-NARX model

The classical Nonlinear Autoregressive with an eXogenous (NARX) input model structure assumes that the output signal of the nonlinear system at a given discrete-time instant t_k can be represented as a function of the past output and input samples of the system. Thinking about nonlinear oscillatory dynamical systems, this means that the displacement $y(t_k)$ of a given point of a structure can be represented as a function of the displacements at past time-instants and the forces applied at past time-instants. In short, we have (Billings, 2013)

$$y(t_k) = \mathscr{F}(y(t_{k-1}),\dots,y(t_{k-n_y}),U(t_k),U(t_{k-1}),\dots,U(t_{k-n_U+1})) + \varepsilon_k^y = \mathscr{F}(\mathbf{x}_k) + \varepsilon_k^y, \tag{1}$$

where $\mathscr{F}$ represents a multidimensional nonlinear function, $\varepsilon_k^y \sim \mathscr{N}(0,\sigma_y^2)$ a zero mean independent Gaussian noise - with variance σ_y^2, $y(t_k)$ the displacement at instant t_k, $U(t_k)$ the input force at instant t_k, n_y the output maximum number of lags, n_U the force maximum number of lags, and $\mathbf{x}_k$ represents a vector of inputs (past samples of displacements and forces) which is taken to output $y(t_k)$ through the nonlinear function $\mathscr{F}$. This framework represents a nonparametric way to represent the output signal without directly knowing the motion equation or the physics of the system in analysis.

The most important question is how to determine the nonlinear relation between the different lags considered on the output signal representation. To overcome this issue, and directly represent the nonlinear function $\mathscr{F}(\cdot)$, many regression machine learning models could be adopted, as for example, Sparse Linear Regression, Neural Networks, Decision Trees, etc. (Bishop and Nasrabadi, 2006). This paper adopts the Gaussian Process Regression (GPR) model (Kocijan, 2016). First of all, consider that we have a training data-set $\mathscr{D} = (\mathbf{x}_k, y_k)_{k=1}^N \equiv (\mathbf{X},\mathbf{y})$, composed by N time-instants t_k. Now, let's consider that the nonlinear function $\mathscr{F}(\cdot)$ is assumed to follow a zero mean multivariate Gaussian prior distribution

$$\mathbf{F} = \mathscr{F}(\mathbf{X}) \sim \mathscr{N}(\mathbf{F}|\mathbf{0},\mathbf{K}), \tag{2}$$

where $\mathbf{K}$ is the covariance matrix with $K_{ij} = k(\mathbf{x}_i,\mathbf{x}_j)$, with $k(\cdot,\cdot)$ representing a *covariance function*, also known as kernel function. The kernel trick is used because is very difficult (almost impossible) to estimate the exact covariance matrix based on data. With a new input vector $\mathbf{x}_*$, using probability rules for the multivariate Gaussian distribution, we can calculate the posterior mean and variance, considering the independent Gaussian noise (Williams and Rasmussen, 2006)

$$\mu_* = k_{*N}\left(\mathbf{K}+\sigma_y^2\mathbf{I}\right)^{-1}\mathbf{y}, \tag{3}$$

$$\sigma_*^2 = k_{**} - k_{*N}\left(\mathbf{K}+\sigma_y^2\mathbf{I}\right)^{-1}k_{N*}, \tag{4}$$

where $\mathbf{I}$ is the identity matrix, related to the covariance matrix of the independent Gaussian noise assumed. Finally, for the correct estimation of the model, we must determine a covariance function and its hyperparameters, the number of lags of the output signal and applied force, and the noise variance. In the estimation of hyperparameters and noise variance, the maximization of maximum likelihood was applied as done in Teloli et al. (2021).

Moreover, for the covariance function and number of lags, the exhaustive search (testing different kernel functions and lags used) was considered. In this work, three different kernels functions were tested:

- The Radial Basis Function (RBF) kernel

$$k(\mathbf{x}_i,\mathbf{x}_j) = \sigma_m^2 \exp\left[-\frac{1}{2l^2}|\mathbf{x}_i-\mathbf{x}_j|^2\right]. \tag{5}$$

- The Linear kernel

$$k(\mathbf{x}_i,\mathbf{x}_j) = \sigma_m^2\mathbf{x}_i^T\mathbf{x}_j. \tag{6}$$

- The Matern kernel (with $\nu = \frac{3}{2}$)

$$k(\mathbf{x}_i,\mathbf{x}_j) = \sigma_m^2\left(1+\frac{\sqrt{3}|\mathbf{x}_i-\mathbf{x}_j|}{l}\right)\exp\left[-\frac{\sqrt{3}|\mathbf{x}_i-\mathbf{x}_j|}{l}\right]. \tag{7}$$

where σ_m^2 is the kernels variance and l the lengthscale, i.e., the hyperparameters of each kernel.

More information aboute GPR model can be found in Williams and Rasmussen (2006).

Damage detection index

The model described above gives not only the mean value for the system's output signal but also the variance for each sample. In this sense, a simple method, based on a distance measurement, can be used to monitor the structural condition while taking model uncertainty into account. In this work, an adaptation of the original standardized Euclidian distance between vectors will be used

$$D(y_{\text{exp}}, \mu_y) = \frac{1}{\sigma(y_{\text{exp}})} \sqrt{\sum_{k=1}^{N_p} \frac{[y_{\text{exp}}(k) - \mu_y(k)]^2}{\sigma_y^2(k)}}, \tag{8}$$

were y_{exp} is the experimental signal, $\sigma(y_{\text{exp}})$ represents the standard deviation of the whole experimental signal (used to normalize the index for different signal amplitudes), μ_y is the mean signal obtained through the GP-NARX model, σ_y^2 is the model variance for each signal sample, and N_p is the number of signal samples. The distance obtained in the reference condition, using training data, can be used to define a threshold for damage detection. If the distance measured for a new experimental signal is higher than the threshold, it is supposed that a structural change affected the system dynamics. This index takes into account both mean fit and model dispersion because a higher nominal distance is accepted in regions with higher model uncertainty (higher values of variance).

NUMERICAL EXAMPLE CONSIDERING A DUFFING OSCILLATOR

Nonlinear system

For the purpose of testing the methodology previously described, we performed a numerical study using the classical asymmetric Duffing oscillator as a benchmark. This system is quite interesting because can describe the nonlinear dynamic behavior of a wide range of different real systems. The motion equation is defined as (Kovacic and Brennan, 2011)

$$m\ddot{y}(t) + c\dot{y}(t) + k_1 y(t) + k_2 y^2(t) + k_3 y^3(t) = U(t), \tag{9}$$

where $m = 0.26$ [kg] is the system equivalent mass, $c = 1.36$ [Ns/m] is the damping coefficient, $k_1 = 5.49 \times 10^3$ [N/m] is the linear stiffness, $k_2 = 3.24 \times 10^4$ [N/m^2] is the quadratic stiffness, $k_3 = 4.68 \times 10^7$ [N/m^3] is the cubic stiffness, and $U(t)$ is the external force in [N]. The displacement, velocity and acceleration are, respectively, represented by $y(t)$, $\dot{y}(t)$ and $\ddot{y}(t)$. The values were chosen based on Villani et al. (2019). The Duffing oscillator was simulated using different types and levels of input (chirp and random force signals), using a Runge Kutta numerical integration method. This system, with the parameters cited above, represents the mechanical nonlinear system in reference condition, i.e., without the presence of damage. The presence of damage was emulated reducing the linear stiffness in 2, 4 and 6 %.

In order to analyze the relationship between the excitation amplitude levels and the nonlinear behavior of the output signal, the time-frequency diagram was calculated using the system's response for a chirp input force with two different levels of excitation, in the region of the resonance frequency, varying the excitation frequency from 15 to 35 Hz in 4 seconds. The results obtained are compared in Figure 1. We can observe that for excitations with a low level of amplitude (Figure 1a - 0.1 [N] of force amplitude) the mechanical system amplifies the oscillation amplitudes only for the excitation frequency and resonance frequency. On the other hand, for excitations with a higher level of amplitude (Figure 1b - 1 [N] of force amplitude) the mechanical system also presents amplification for frequencies that are multiples of the resonance frequency (two and three times the resonance frequency). This behavior is characteristic of systems with nonlinearities that present input amplitude dependence, such as the Duffing Oscillator, leading to the breaking of the superposition principle.

Finally, this study will consider not only deterministic inputs, like the chirp force but also the use of random forces applied. In order to parameterize the random signal and generate a force with the same energy as the chirp input, the Root Mean Square (RMS) value was compared for both signals, resulting in an RMS(Root Mean Square) of 81 [mN] for the random force equivalent to an excitation level of 71 [mN] for the chirp force and an RMS of 540 [mN] for the random force equivalent to an RMS of 707 [mN] for the chirp input. These values determined will be considered in the rest of the paper as a reference for low-level and high-level input forces. Whenever results are compared using different input signal types the RMS value will be used to calculate the equivalent force amplitude for each input type. This is an attempt to standardize the results obtained for different input types. The next section shows the results obtained using the proposed methodology for damage detection.

Numerical results

As mentioned before, in this work we applied the GP-NARX model as baseline nonlinear model. This means that once estimated, the model should be able to predict the dynamic behavior of the nonlinear system for new inputs and under unknown structural conditions. However, to define the parameters of the GP-NARX prediction model, we first need to define a kernel function and the number of input and output delays to be considered. For doing so, an exhaustive search strategy was used. We have estimated the GP-NARX model considering the three types of kernel function described

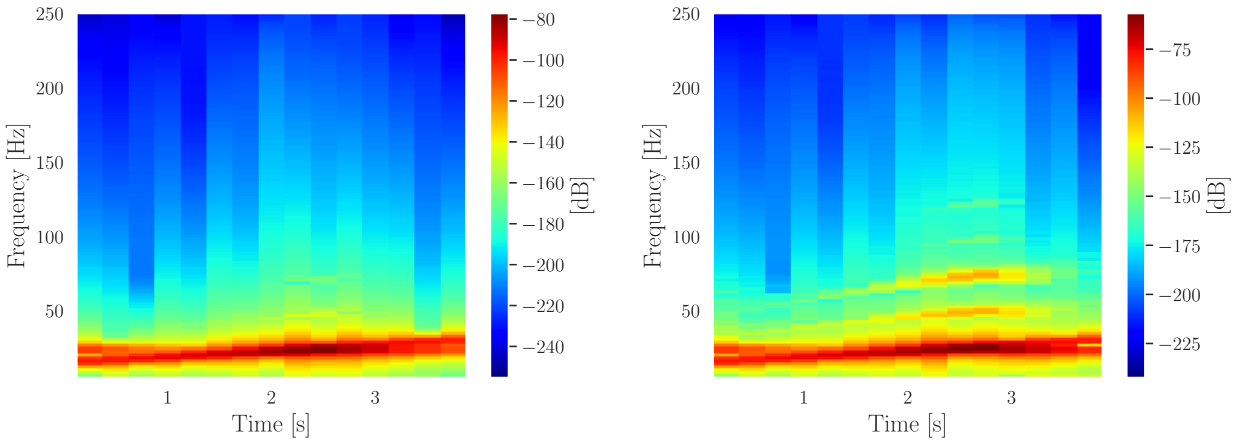

(a) Using a low-level of excitation amplitude (0.1 N).

(b) Using a high-level of excitation amplitude (1 N).

Figure 1 – Time-frequency diagram for different output signals.

before, constructing different combinations of delays (in the range 2 - 16) for the input/output signals. Then, we calculated the percentage of fit obtained using the model, for the data used to train the model plus a control data sample (an output signal obtained for a different excitation). At this point, we considered as training data the system output for a low-level chirp signal (RMS = 71 [mN]) plus a high-level chirp signal (707 [mN]), both varying the excitation frequency from 1 to 35 [Hz] in 4 seconds and as the control sample the output signal obtained for a high-level random signal (540 [mN]), in the same frequency range. In all simulations hereafter, we consider adding white noise at the output of the integrator with a level of 5% of the energy of the output signal obtained for the low-level chirp input signal.

The results obtained during the exhaustive search are displayed in Figure 2 for the kernels: Linear (Figure 2a), RBF (Figure 2b), and Matern 3/2 (Figure 2c). The percentage of fit displayed refers to the mean fit obtained considering the three types of output signal used. The best correlation between higher accuracy and lower computational expense was observed on the combination of 3 delays for the input signal and 11 delays for the output signal using the RBF kernel (Figure 2b), with the mean fit between the three signals evaluated, equal to 96.65 %. This result was considered satisfactory at this point, and this model setup was used for all the other simulations performed. Additionally, in order to observe the model prediction using this configuration, and the model variance (model uncertainty), Figure 3 shows the results obtained when we consider a high-level chirp signal (Figure 3a) and a high-level random signal (Figure 3b) as system excitation, and the model prediction variance calculated for both signals, Figures 3c and d, respectively. The small prediction error demonstrates the model's ability to predict the system output, meanwhile, the variance presents higher values in regions with higher vibration amplitude.

It is known, in general, that machine learning methods are very good in interpolations, but bad in extrapolations. In this sense, it becomes important to study and interpret the range of applicability of the reference model identified. Aiming to identify a valid range of applicability of the damage detection based on the estimated GP-NARX model, using random and chirp excitations, different levels of input amplitude were simulated and the model prediction was calculated. Figure 4 shows the results obtained, considering the mean fit value obtained for a large number of runs. Analyzing the results shown in Figure 4a, it is observed that the model is able in producing good estimations of the system's response from $\approx$ 71 [mN] up to 707 [mN], with a fit upper than 95%, for chirp input signals. That was exactly the range used to train the model. For excitations with higher amplitude, the performance starts to degrade as the nonlinearity increases its contribution to the total response (fit values lower than 95%). For the random excitation (Figure 4b), similar behavior is observed, the difference is related only to the range of amplitudes, because the effect of energy concentration close to the resonance frequency is different for random and chirp inputs. This test shows that the estimated model works very well, respecting the limits used in the training phase, which is not always respected in practical applications where the input is not controlled (a clear limitation of the methodology).

With the reference model estimated, the nonlinear system was simulated using different inputs (type and amplitude level) and damage conditions, represented by linear stiffness reduction. Remembering that, a white noise with 5% of the standard deviation of the low-level amplitude chirp input signal was added in each simulated signal. Additionally, for each condition simulated the calculations were repeated 200 times, to include the noise and random signal variabilities in the analysis. For each simulation, the distance index was calculated using Eq. 8 and the results obtained are analyzed as follows.

Figure 5 shows the results obtained for the distance index calculated when we consider the system in the reference condition, but by applying different kinds of input. By analyzing the damage indices presented by the model in each case it can be seen that for the amplitudes closer to the chirp signal with high amplitude the influence on nonlinearities was better fitted, which has been shown by the lower damage indexes presented when compared to both the lower excitation signals between the high and low training inputs and the higher signal above the high training signal (Figure 5a). Although the lower chirp signals have presented indexes up to 30 (5 times bigger than the mean obtained for the higher chirp signals), caused by the high magnitude of the noise when compared to the main signal, those still have been presented small when compared to the damage indices obtained for the samples with simulated damage (with the lower mean damage index being 170 for the 2% damage condition with the random input and the minimum damage index being equal to 100 on a unique sample, as can be seen on Figures 6 and 7, discussed further). Furthermore, this condition is assumed to be known, i.e. a threshold value can be established based on this data in the reference condition. On other hand, the signals that exceeded the training amplitudes showed much more scattered data (mainly for the random input), which can hinder damage detection. Confirming that a range needs to be established for a safe operation of the methodology, reducing the number of false alarms. Another strategy might be to recalibrate the model as the number of false positives grows.

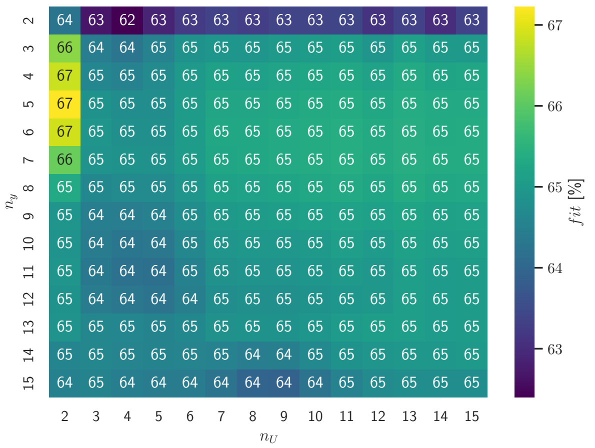

(a) Linear kernel.

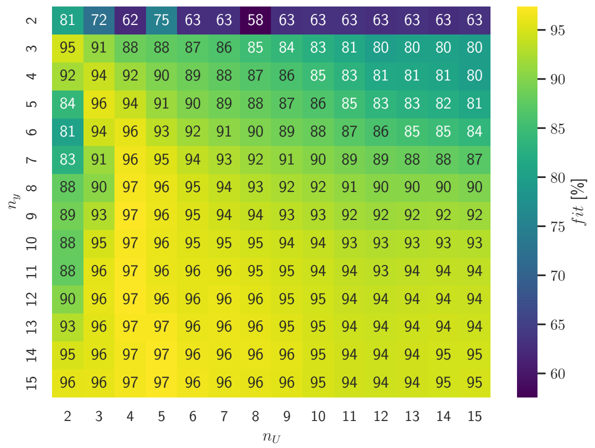

(b) RBF kernel.

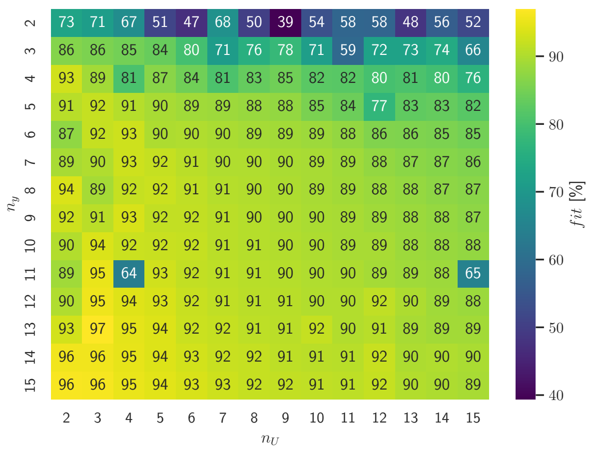

(c) Matern 3/2 kernel.

Figure 2 – Prediction error calculated using different types of kernels and number of input/output delays.

Lastly, Figures 6 and 7 presents the results obtained considering simulated damage in the analysis. The damage represents small losses of stiffness in the system. It can be seen that, for all the cases considered, the calculated distance index increases rapidly with the appearance of damage, showing a high level of sensitivity to the presence of structural variation. As expected, the data calculated considering random input is more dispersed, while deterministic input with concentrated energy is more sensitive to the presence of damage. On the other hand, these inputs excite more nonlinearities, and changes in excitation amplitudes can be easily confused with the presence of damage, as commented earlier. Finally, since the amplitudes of the indices calculated in conditions where damage is present are of much higher numerical order than those calculated from the variation in excitation amplitudes, it can be said that the methodology is promising to be applied to systems with intrinsically nonlinear behavior still in healthy conditions.

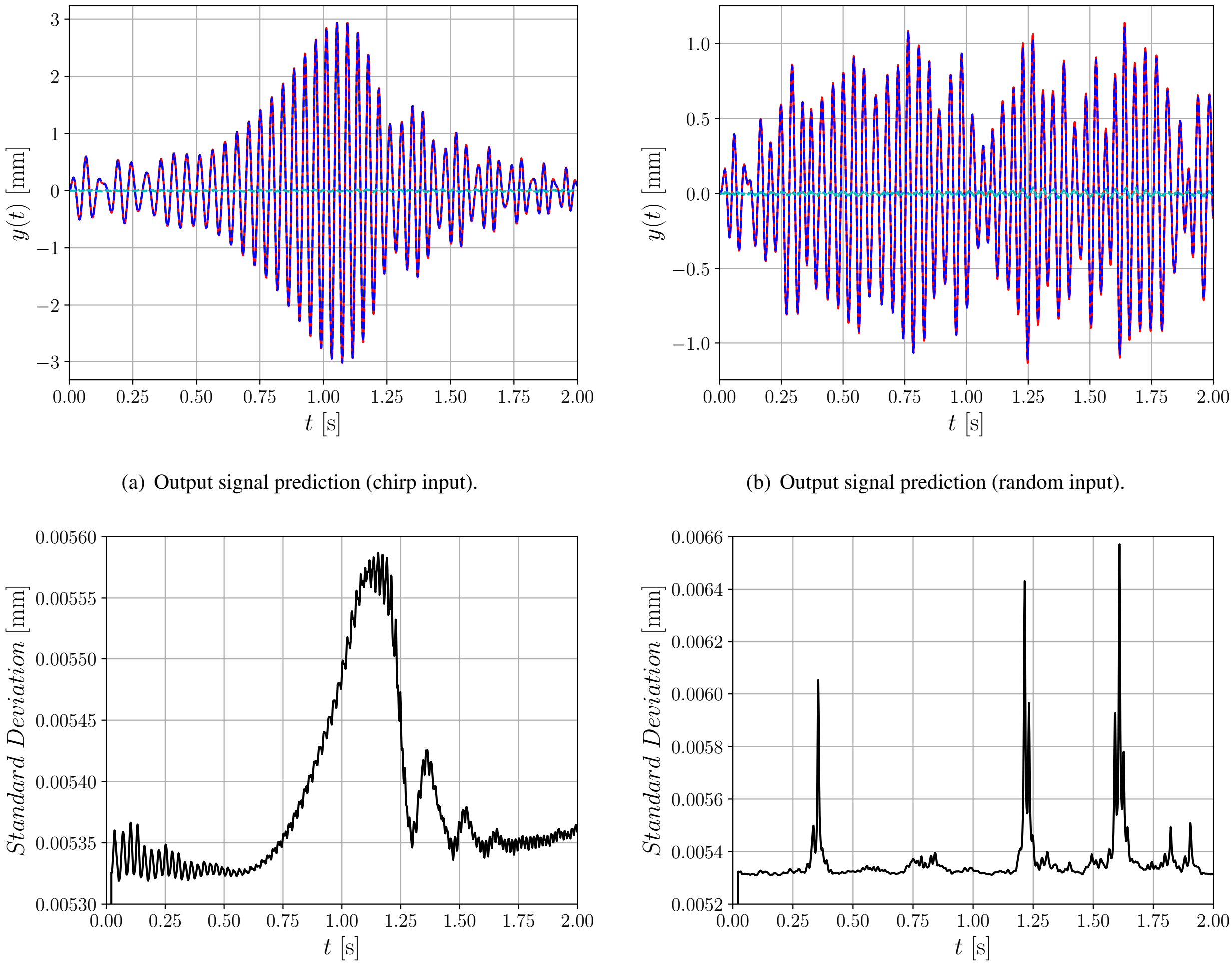

(a) Output signal prediction (chirp input).

(b) Output signal prediction (random input).

(c) Model prediction variance (chirp input).

(d) Model prediction variance (random input).

Figure 3 – Model prediction for different kinds of input signal, both considering a high level of amplitude. Blue represents the mean model output, red the simulated output and cyan the prediction errors, black shows the variance of the model.

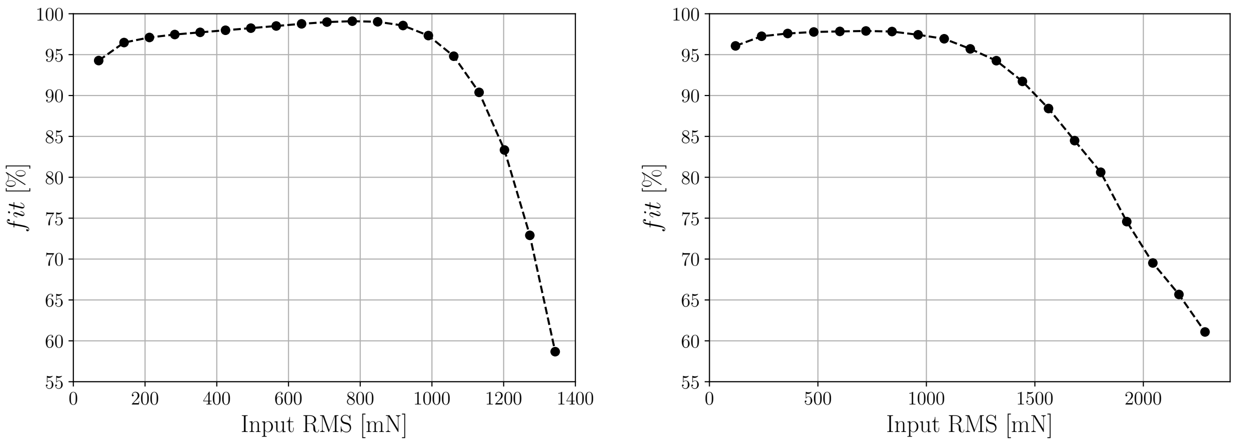

(a) Chirp input.

(b) Random input.

Figure 4 – Fit values with input signal amplitude variation.

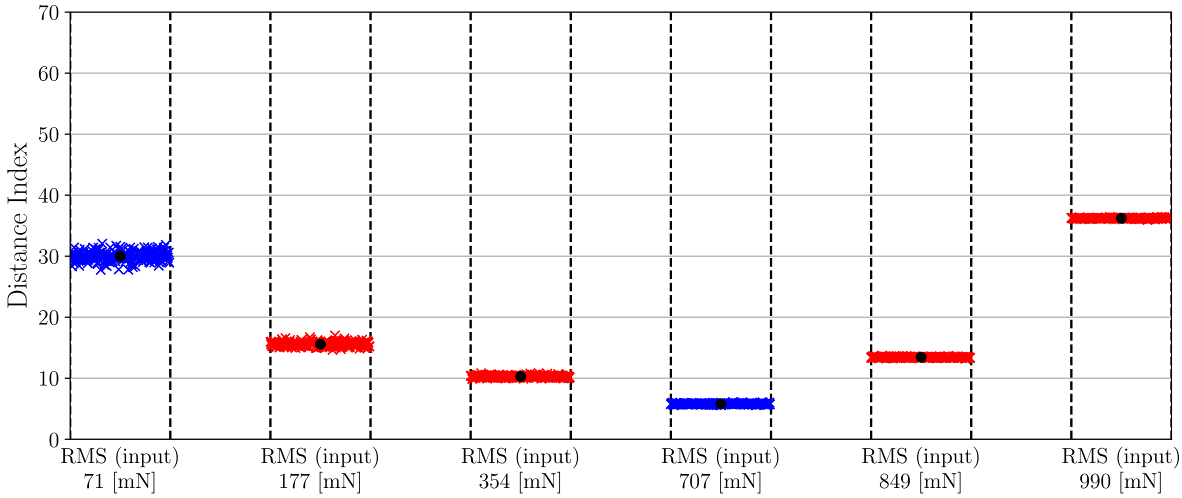

(a) Chirp input.

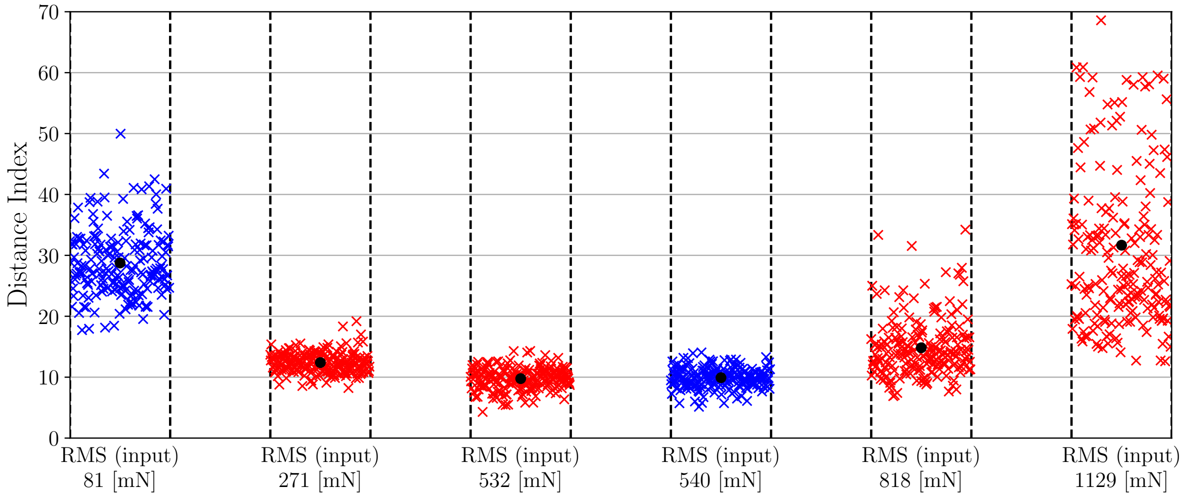

(b) Random input.

Figure 5 – Distance index variation with input signal amplitude variation. Blue refers to the amplitudes used in the training phase.

FINAL REMARKS

A damage detection methodology based on a nonlinear reference model has been proposed and tested considering a Duffing oscillator as a benchmark. Using this methodology, conditions considering different types of the input signal, at different amplitude levels, were tested. Structural variation was simulated by stiffness reduction. The results observed throughout the simulations showed promise, but special attention should be given to the validation of the reliable operating limits of the GP-NARX model since, like all machine learning models, it proved to be a good interpolator but left a lot to be desired in the extrapolation of the behavior of the nonlinear system.

For future work, the authors suggest studies using experimental data and the use of models that can improve their performance from the insertion of knowledge of the physics involved in the phenomenon. It is hoped that a little physical knowledge added to the model may allow a greater ability to extrapolate predictions to the machine learning-based method.

ACKNOWLEDGMENTS

The authors are grateful for the support of Universidade Federal do Espírito Santo (UFES) and Conselho Nacional de Desenvolvimento Científico e Tecnológico (CNPq) for funding this research.

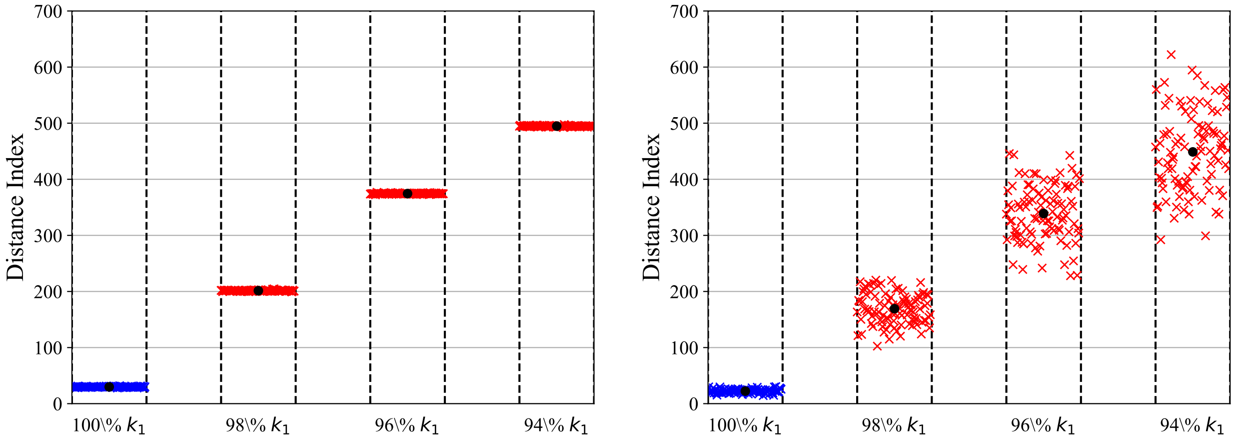

(a) Chirp input (0.1 [N]).

(b) Random input (0.4 [N]).

Figure 6 – Distance index variation with structural variation for low-level excitation. Blue refers to the reference condition (without damage).

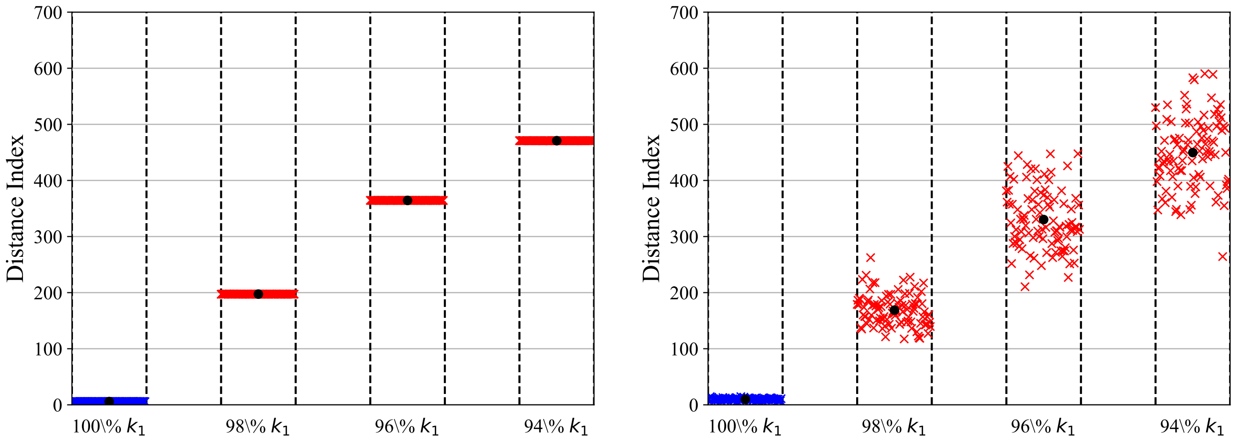

(a) Chirp input (1 [N]).

(b) Random input (2 [N]).

Figure 7 – Distance index variation with structural variation for high-level excitation. Blue refers to the reference condition (without damage).

REFERENCES

Billings, S. A. (2013). *Nonlinear system identification: NARMAX methods in the time, frequency, and spatio-temporal domains*. John Wiley & Sons.

Bishop, C. M. and Nasrabadi, N. M. (2006). *Pattern recognition and machine learning*, volume 4. Springer.

Kerschen, G., Worden, K., Vakakis, A. F., and Golinval, J.-C. (2007). Nonlinear system identification in structural dynamics: current status and future directions. In *25th International Modal Analysis Conference, Orlando, 2007*.

Kocijan, J. (2016). *Modelling and control of dynamic systems using Gaussian process models*. Springer.

Kovacic, I. and Brennan, M. J. (2011). *The Duffing equation: nonlinear oscillators and their behaviour*. John Wiley & Sons.

Teloli, R. O., Villani, L. G. G., da Silva, S., and Todd, M. D. (2021). On the use of the GP-NARX model for predicting hysteresis effects of bolted joint structures. *Mechanical Systems and Signal Processing*, 159:107751.

Villani, L. G. G., da Silva, S., and Cunha Jr, A. (2019). Damage detection in uncertain nonlinear systems based on stochastic Volterra series. *Mechanical Systems and Signal Processing*, 125:288–310. Exploring nonlinear benefits in engineering.

Williams, C. K. I. and Rasmussen, C. E. (2006). *Gaussian processes for machine learning*, volume 2. MIT press Cambridge, MA.

Worden, K., Becker, W., Rogers, T., and Cross, E. (2018). On the confidence bounds of Gaussian process NARX models and their higher-order frequency response functions. *Mechanical Systems and Signal Processing*, 104:188–223.

Worden, K., Kerschen, G., Vakakis, A. F., and Golinval, J.-C. (2007). Nonlinear System Identification in Structural Dynamics: A Short (and Biased) History. In *25th International Modal Analysis Conference, Orlando, 2007*, pages 1996–2017.

RESPONSIBILITY NOTICE

The authors are the only responsible for the printed material included in this paper.